Acc. Chem. Res. **2000,** *33,* 475−481

A Dynamic View of Self-Assembled Monolayers

ANTONELLA BADIA,† R. BRUCE LENNOX,‡ AND LINDA REVEN*

Department of Chemistry, McGill University, 801 Sherbrooke Street West, Montreal, Quebec, H3A 2K6 Canada

Received February 9, 1999

ABSTRACT

In this Account, we discuss the dynamic features of self-assembled monolayers (SAMs) on both planar and nonplanar substrates. Our focus is on organothiol and organic acid-based monolayers. Results from variable-temperature electrochemical, calorimetric, vibrational, and solid-state NMR spectroscopic measurements lead to a convergent description of SAM dynamics.

Introduction

This Account specifically addresses issues relating to the dynamics of self-assembled monolayers (SAMs) formed on both planar (2D) and particle (3D) surfaces. In addition to fundamental issues in surface chemistry, SAMs are of interest for applications in corrosion control, device fabrication, and membrane mimicry.[1,2] How chain mobility and order affects the functional properties of SAMs (as electron-transfer barriers and adhesion and wetting modifiers) is difficult to address since techniques which probe molecular motion, such as NMR, cannot be used for planar SAMs.

Discussions of structure and dynamics in molecular assemblies obviously involve discussions of phase.[3] The phase behavior of 2D SAMs reported by various techniques, however, depends on whether the technique is sensitive to positional, orientational, or conformational order (or combinations thereof). We have been particularly interested in how these factors are coupled to one another and how one can deconvolute and prioritize them with regard to the self-assembly process and chain-ordering phenomenon. The mainstay of phase studies, calorimetry, is of limited utility when one is dealing with only 10^{-10} mol of material. The experimental signal-to-noise problem has been addressed in several ways. A technique that is sensitive to the structure of the SAM and uses some form of signal amplification (i.e., amperometic electrochemistry) can be used.[4] Alternatively, one can scale-up the planar ("2D") substrate surface area by $>10^4$-fold by using nanoparticles[5] so that techniques such as calorimetry,[6,7] transmission IR spectroscopy,[6,8,9] and, most notably, dynamic NMR spectroscopy[10] can be used. Finally, state-of-the-art STM and AFM techniques can often provide a visualization of phases.[14a] Most SAM studies actually report the static features of either ordered or disordered phases (rarely both), but not their dynamics.

This Account will focus on the dynamics of chains in SAMs of alkylthiols on gold (RS/Au) and long-chain organic acids (RCO_2H, RPO_3H_2) on metal oxides.[11] Although alkylthiols and fatty acids are not usually compared, we find that they display similar properties and are thus complementary. The dynamic features we have observed are closely associated with the surface-tethered chains and not with the substrate surface nor the chemistry of the headgroup. After a brief overview of the relevant literature, we describe the electrochemical, calorimetric, and spectroscopic studies of these systems which present a picture of SAM dynamics.

2D SAMs of Alkanethiols and Long-Chain Organic Acids

SAMs of organosulfur adsorbates, especially alkanethiols (RSHs) on gold surfaces, have been the most studied.[1,2] The ordering of alkanethiols is driven by the strong affinity between the sulfur and the metal, the lateral van der Waals interactions between the tethered alkyl chains, and the dipole interactions between polar end groups. The structure of 2D SAMs is characterized by both positional and orientational order. The positional order is fixed by the headgroup binding at particular sites on the substrate surface and whether the chain lies flat on the surface or adopts some vertical orientation. Positional order, however, does not necessarily imply the existence of orientational order (and vice versa). Given that the gold−sulfur binding energy (∼160 kJ/mol)[2] is much larger than the alkyl chain−chain interactions (of the order of tens of kilojoules per mole),[12] the sulfur headgroups may exist in ordered lattices at the same time that the alkyl chains may be orientationally and conformationally disordered. High gap impedance UHV−STM images show that the alkylthiolates exist in as many as six phases, each having a particular positional order.[15b] A SAM formed on a single-

Antonella Badia received her Ph.D. from McGill University in 1996. After postdoctoral studies at the Max Planck Institute for Polymer Research (Mainz, Germany) and the McGill Center for the Physics of Materials, she joined the faculty of the Université de Montreal in 1999. Her research interests include organic ultrathin films, chemical force microscopy, and micromechanical cantilever sensors.

Bruce Lennox carried out his undergraduate and graduate studies at the University of Toronto (Ph.D., 1985). He joined the Chemistry Department at McGill University in 1987 after postdoctoral studies at Imperial College (London, UK) with John Albery. He is a member of PENCE (Protein Engineering Networks of Centre of Excellence) and an Associate Member of the McGill Center for the Physics of Materials. His research interests span the fields of interfacial chemistry, nanostructured materials, bioelectrochemistry, and physical organic chemistry.

Linda Reven obtained a B.A. from Carleton College, Northfield, MN. Her doctoral studies were carried out with Eric Oldfield at the University of Illinois, Urbana (Ph.D., 1990). After postdoctoral studies with Alex Pines at the University of California at Berkeley, she joined the faculty at McGill University. She is currently spending a sabbatical year at the Max Planck Institute for Polymers (Mainz, Germany). Her research focuses on solid-state NMR methods for the structural and dynamic characterization of self-assembled monolayers, adsorbed polymers, and polymer micelles.

* To whom correspondence should be addressed. E-mail: linda_reven@maclan.mcgill.ca.

† Present address: Département de chimie, Université de Montréal, C.P. 6128, succursale Centre-ville, Montréal, Québec, H3C 3J7, Canada. E-mail: antonella.badia@umontreal.ca.

‡ E-mail: bruce_lennox@maclan.mcgill.ca

10.1021/ar9702841 CCC: $19.00
Published on Web 03/23/2000

crystal substrate has a number of discontinuities along-coexistence lines and adjacent to defect points and etch pits.[13−16]

Infrared spectroscopy is particularly useful for characterizing the state of the alkyl chains. A comparison of the antisymmetric $\nu_a(CH_2)$ peak frequencies of RS/Au SAMs ($R = C_4-C_{22}$) shows a trend to lower peak frequencies as R increases in length. When $R \geq C_{16}$ the monolayer exists in a crystalline-like, all-trans state, whereas for $R \leq C_8$ the local environment of the alkyl chains approaches that of the bulk disordered, liquidlike state.[17] Long-chain RS/Au SAMs are not perfectly crystalline, given that the He diffraction intensities at 25 °C show that the chain ends are highly mobile and disordered.[18] Molecular dynamics simulations predict that at temperatures <−75 °C, the chains are orientationally ordered, collectively tilted in the nearest-neighbor direction, and free of gauche defects. At 27 °C, the simulations indicate that the chains are rotated about their long axes and a significant population of conformational defects is located at the chain ends.[3] In addition to chain-disordering processes, temperature-induced reconstructions of the SAM/Au interface,[19−21] nucleation and growth of ordered domains induced by the partial desorption of surface thiolates,[14a,16,22] and surface migration of the RS/Au species[21,23−25] have also been observed.

Long-chain organic (carboxylic, hydroxamic, phosphonic) acids on metal oxides are a class of SAMs which have been studied to a much lesser extent than the thiols on gold. Alkanoic acids on oxides of silver, aluminum, and other metals were actually among the first SAMs to be reported.[26] These SAMs have been used for model studies of corrosion inhibition[27] and as a bridge between SAM and LB studies.[26b] The organic acid surface bond is more ionic than the Au−S bond, and the fatty acid monolayers are less stable. As in the case of the thiols, most reports to date focus on static structural features such as the variation of the binding geometry with the type of metal oxide.[27a] A recent ESR study of stearic acid SAMs on Al_2O_3 did, however, show that the onset of rotational motion depends on the location of the spin label along the chain.[28]

Phosphonic acids bind more strongly to metal oxide surfaces than do carboxylic acids. Multilayer assemblies, based on lamellar metal phosphonate structures, have been grown on a variety of substrates.[29] The chain conformation and growth kinetics of long-chain phosphonic acid monolayers on mica[30] and aluminum surfaces[31] have been monitored by atomic force microscopy (AFM) and FT-IR spectroscopy. The growth mechanism on mica consists of nucleation, slow growth, and coalescence of islands in which the chains are densely packed and relatively well-ordered even at a low surface coverage.[30c] An FT-IR study of the self-assembly of phosphonic acids on alumina revealed that although the initial adsorption is rapid, the chain order develops quite slowly over several days.[31] As in the Au/SR system, sensitivity problems have made it difficult to use the time-resolved techniques which provide dynamics information.

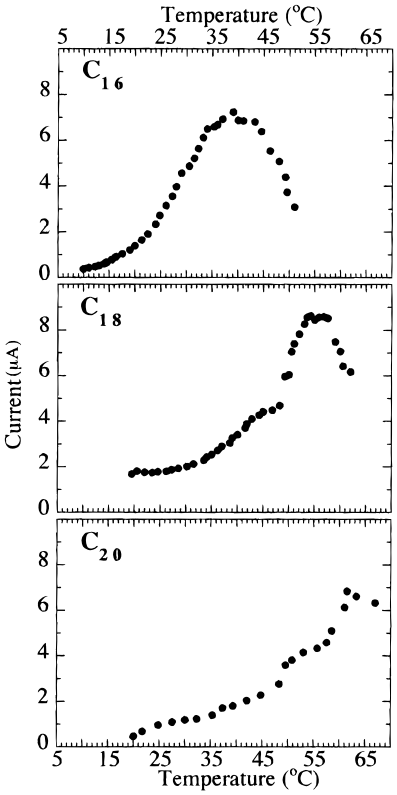

FIGURE 1. Electrochemical thermograms (current vs temperature) for the reduction of $Fe(CN)_6^{3-}$ (0.020 M, 0.10 M KBr) at RSH-modified polycrystalline gold electrodes. The current is reported at an overpotential of −0.25 V. (Adapted from ref 4).

Effect of 2D SAM Dynamics on Function: Electrochemical Studies

How can dynamics within the SAM manifest themselves in terms of function? We have explored one configuration in detail and have observed a striking correspondence between the onset of chain motion, phase disordering, and ion flux across RS/Au SAMs.

The experiment is similar to many electrochemical studies of SAMs[32] but differs in terms of SAM preparation. We prepare RS/Au SAMs (where a polycrystalline gold surface is incubated in RSH/EtOH solution) in a manner different from that used by most researchers in that we maintain the incubation at modest temperature for periods of days. Although complete coverage takes only minutes to achieve with an RSH solution, the dynamics of chain ordering are very slow. We have used our electrochemistry technique to monitor this process; recent in situ SECM experiments provide a time-dependent visualization of it as well.[33] As the temperature is slowly increased from 25 °C, the ion flux increases markedly, goes through a maximum at T_m^e (often with a shoulder on the low-temperature side, T_p^e) and then subsequently decreases to a level which is generally greater than that prior to the maximum (Figure 1). The temperatures at which both the "shoulder" (or prepeak) and the main peak appear increase incrementally with chain length. What is striking is the 1:1 correspondence between (i) the temperatures of these maxima in the SAM electrochemical experiment,[4] (ii) the DSC-, FT-IR-, and NMR-determined

Table 1. Transition Temperatures and Enthalpies for RS SAMs on Planar Gold, Au Nanoparticles, and Related Lipids

	RS/Au planar (electrochemical)	RS/Au nanoparticles		di-PC lipids	
R	T_m^e (°C)	T_m (°C)	ΔH (kJ mol^{-1})	T_m (°C)	ΔH^a (kJ mol^{-1})
C12	−	3	6.4 ± 2.5^b	-1.1 ± 0.4	6.1 ± 3.4
C14	−	22	10	23.5 ± 0.4	12.4 ± 1.4
C16	39.3 ± 0.6	41	13.8 ± 0.8^b	41.4 ± 0.5	17.4 ± 1.6
C18	53.3 ± 2.4	51	21	55.1 ± 1.5	21.2 ± 1.8
C20	62.8 ± 1.8	64	−	64.5 ± 0.5	24.9 ± 1.2

[a] For comparison with the alkylthiolates, the ΔH values (ref 12 for the diacyl phospholipids) are reported per alkyl chain. [b] ΔH values are from ref 7.

order−disorder phase transition temperatures of the 3D SAMs,[6,9,10] (see below) (iii) the gel-to-liquid crystalline (order−disorder) phase transition temperatures of phosphatidylcholine phospholipids in the bilayer state,[12] and finally, (iv) the temperatures at which anomalous maxima in ion permeation rates across bilayer lipid membranes occur[32] (Table 1). These correlations are consistent with the maxima in lipid ion permeation studies arising from a great enhancement of redox ion transfer at domain and phase boundaries. These boundaries would occur at coexistence regions between ordered and disordered domains in the membrane.[34]

The phospholipid headgroup in a bilayer membrane and the Au lattice apparently serve the same purpose—to enforce a defined packing density and orientation on the alkyl chains. In RS/Au(111) SAMs, the area occupied per RS chain is 21.7 Å^2, and the alkyl chain tilt is ∼30° (from the surface normal).[2] By comparison, *n*-diacylphosphatidylcholines occupy an area of 21.5−24 Å^2 per alkyl chain in their condensed phase and exhibit a chain tilt of ∼30° from the bilayer normal.[12] It is therefore reasonable that the structural film properties in these two systems are modulated by temperature in a similar manner.

Complexities of the relationship between chain dynamics and phase in RS/Au SAMs are further evident in these temperature-dependent electrochemistry studies. SAMs which have not had the opportunity to form ordered phases (because of insufficient incubation time or heterogeneities in the underlying substrate) do not exhibit the current maxima shown in Figure 1. Furthermore, after an RS/Au SAM has been heated above T_m^e, its return to an ordered state can take hours or days. The kinetics of chain crystallization (or recrystallization) are very slow, probably because of chain entanglement and restricted lateral chain movement. As in RS/Au SAMs, thermal annealing of solid-supported fatty acid Langmuir−Blodgett (LB) monolayers causes disorder in the alkyl chains which is long-lasting (>6−10 h).[35] UHV−STM studies of SAMs (R = C_8, C_{10}, and C_{12}) have shown that the thermal annealing of film defects and the concomitant increase in the alkanethiolate domain size occur at the same temperature as the onset of alkanethiolate desorption.[14a,16,36] These results are in marked contrast to the usual perception of an annealing process in which heating at temperatures close to the melting point usually improves the chain order. We now realize that one must be very cautious in the thermal treatment of a 2D SAM sample if one is seeking phase or dynamics-related properties as the "reordering" process can be slow, and actually sometimes very difficult to effect.

3D SAMs: RS/Au Nanoparticles and Long-Chain Organic Acids on Metal Oxide Particles

SAMs prepared on small particles ("3D SAMs") are important in understanding structure and dynamics issues of the "2D" SAMs.[37] The sampling limitations imposed by planar SAMs are circumvented by the large surface area (ca. 100 m^2/g). One of course has to establish that a SAM formed on nanoparticles is, indeed, representative of the 2D SAMs. A number of pieces of evidence for the RS/Au system tell us that the comparison is, indeed, viable. Powder X-ray diffraction and high-resolution transmission electron microscopy (TEM) studies show that the alkanethiol-capped Au nanoparticles are highly faceted and, hence, that the substrate surface is actually planar and not curved at the local level.[38] Interparticle distances and DSC results indicate that there is an extensive intercalation of bundles of chains between neighboring particles.[6] High-resolution XPS demonstrates that the Au−S bonding is the same in the two systems when the particles are >2.2 nm in diameter. Highly ordered long-chain organic acid SAMs (phosphonates, carboxylates) can also be formed on powdered metal oxides.[39] The average metal oxide particle size (30 nm) is much larger than in the case of the gold nanoparticles (2−3 nm). The organic acid chains in this case do not extensively interdigitate between adjacent particles.

Differential scanning calorimetry (DSC) of RS/Au nanoparticles demonstrates that the chains adsorbed onto Au (R = C_{12}−C_{20}) clearly undergo distinct *T*-dependent phase transitions (Table 1).[6] Each sample exhibits a broad endotherm in the heat cycle. Both the peak temperature and ΔH_{endo} increase with increasing chain length. On cooling of the sample, a sharp exotherm is observed. This exotherm occurs at ∼7 °C lower than the endotherm. Although this hysteresis is observed with all the RS/Au samples studied, the thermal processes are reversible, given that $\Delta H_{exo} = \Delta H_{endo}$ and that $\Delta H_{endo}{}^{heat} = \Delta H_{endo}{}^{reheat}$.

Chain Conformation in 3D SAMs: FT-IR and ^{13}C NMR Spectroscopy

One can readily use conventional transmission FT-IR spectroscopy to study the long-chain organic acid SAMs on the powdered metal oxide and the RS/Au nanoparticles.[6,8] The frequency and width of the methylene stretching adsorptions indicate that for R ≥ C_{16}, the alkyl chains of these two systems exist predominantly in an extended, all-trans conformation at 25 °C. Variable-temperature transmission FT-IR studies show that the RS/Au (C_{14}, C_{16}, and C_{18}) nanoparticles undergo a change from a highly chain-ordered state to a chain-disordered state, where both ν_s (CH_2) and ν_a (CH_2) increase by 2−4 cm^{-1}.[6] The transition temperatures are similar to those found by DSC. As in the DSC experiments (and NMR experiments,

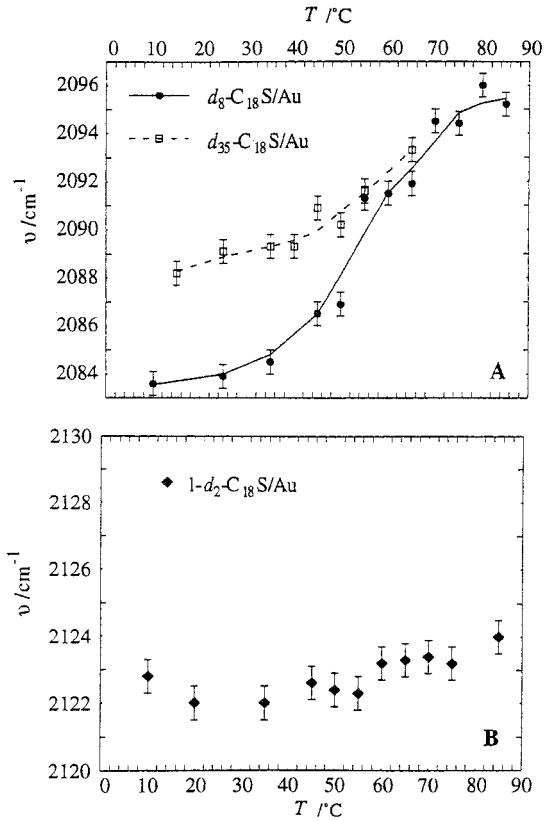

FIGURE 2. Relationship between IR peak position of the symmetric CD_2 stretch and temperature for (a) 10,11,12,13-d_8-C_{18}S/Au nanoparticles and d_{35}-C_{18}S/Au nanoparticles and (b) 1-d_2-C_{18}S/Au nanoparticles. (Reference 9.)

see below), the FT-IR transition occurs over a broad temperature range (~25 °C). This is reminiscent of the DSC and electrochemistry results. Both the endotherm in the RS/Au colloidal system and peaks in the electrochemical thermogram in 2D RS/Au SAMs are broad, spanning as much as 40 °C.[4] Broad transitions are characteristic of 2D systems (LB systems, polymerized lipid membranes, lipid membranes on glass spheres)[41,42] and are a signature in both 2D and 3D SAMs of melting in quasi-2D systems.

Site-specific deuterium labeling of the alkylthiol chains reveals that the gradual shift in ν_s and ν_a with increasing temperature occurs because the IR experiment reports a weighted average of the trans and gauche bond populations along the entire chain length (Figure 2).[9] C_{18}S/Au nanoparticles, whose chains have been deuterated only from C_{10} to C_{13}, show a much sharper disordering transition than particles derivatized with perdeuterated C_{18}SH. The C_1-deuterated position does not, however, undergo a change between 10 °C and 90 °C. The local order is thus maintained at the C_1 carbon, while the remainder of the chain undergoes motions leading to disordering. Site-specific labeling is clearly necessary in distinguishing between ordered and disordered states in the chains. The selective deuteration results tell us that the broadness noted in the calorimetry experiment arises because the chain-disordering process is a progressive process, from chain terminus down, rather than the characteristic "all-or-nothing" process of a first-order transition. With this revealed, we turned to NMR techniques which could track

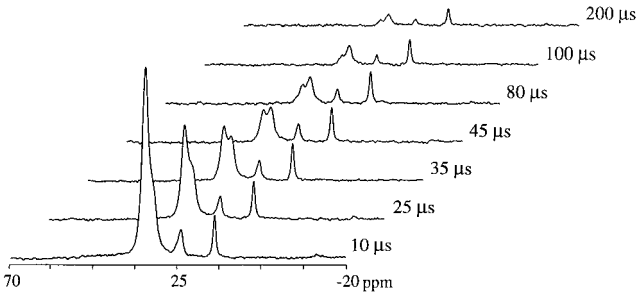

FIGURE 3. Solid-state ^{13}C dipolar dephasing NMR experiment of octadecanethiol monolayers on Au nanoparticles shown as a function of increasing dephasing times. (Reference 10b.)

the dynamics of individual positions along the tethered chains.

Solid-state ^{13}C NMR spectroscopy results corroborate the FT-IR information, since populations of ordered and disordered chains can be distinguished and quantified. In some cases, well-resolved peaks are observed since the ^{13}C resonances for all-trans extended chains are shifted downfield from chains containing gauche defects. The NMR experiment goes much further, though, as the ordered and disordered regions in the SAM can also be resolved on the basis of varying mobilities, using the dipolar dephasing experiment on C_{18}S/Au 3D SAMs (Figure 3) performed at 25 °C.[10b] This experiment probes how the $^{13}C-^{1}H$ heteronuclear dipolar interaction is averaged by molecular motion. The 33 ppm signal (arising from the all-trans chains) rapidly dephases to reveal a signal at 31 ppm assigned to more mobile chains which contain a larger number of gauche conformers. A large motional gradient along the chain is evident in these experiments, as the inner methylenes exhibit a short, solid-like Gaussian decay whereas the chain ends exhibit a long exponential decay characteristic of liquid-like dynamics. An analysis of the chemical shifts and integrated intensities of the methylene resonances establishes that 74% of the chains have transoid segments (containing ~2% gauche bonds) and 26% have gauchoid chain segments (containing ~30% gauche bonds). A total population of 12% gauche bonds is thus present at 25 °C. This seems to contradict the FT-IR results, which report that only highly ordered chains exist at this temperature.[6,8,9] A contributing factor to this discrepancy arises because IR spectroscopy involves an extremely short time scale (ca. 10^{-10} s) and reports a sample-averaged signal, whereas ^{13}C NMR involves the μs time scale. Whereas the "instantaneous" population of gauche bonds is evidently below the detection limit of FT-IR, over the μs time scale of the NMR experiment, many of the bonds will have adopted a gauche conformer. Furthermore, the FT-IR peak maxima alone are normally reported without the line widths, which also contain conformation information.

Variable-temperature, solid-state ^{13}C NMR also reveals that long-chain organic acid SAMs on metal oxide powders and RS/Au nanoparticles undergo disordering transitions which span a broad temperature range.[10,39] In the case of C_{18} chains, thermal chain disordering manifests itself as the gradual growth of the 31 ppm peak (due to

an increase in the gauche conformers) and a diminishing of the all-trans peak at 33 ppm. Above 60 °C, the 33 ppm component is almost completely gone. The chain-disordering process is reversible as the ^{13}C NMR spectrum returns to its original, trans-dominated state upon cooling of the sample to 25 °C. For a given chain length, the chain-disordering process occurs over the same temperature range in the alkylthiol, phosphonate, and carboxylate 3D (and when measurable, 2D) SAMs. We note that the chain dynamics may not apply to an ideal, single-phase SAM on a single-crystal surface. The free volume required for the motional states of the pinned chains is provided by large headgroups and/or surface defects. Although the dynamic features of an ideal, single-phase SAM may, in fact, be different, we propose that the real, defect-containing systems (such as SAMs on polycrystalline gold) will display the dynamics features outlined above. Because these order−disorder transitions clearly are a general feature of both 2D and 3D SAMs, we were compelled to attempt experiments which can explicitly study the evolution of the disordered state from a chain dynamics point-of-view.

Wide-Line NMR Studies of Chain Mobility: ^2H and 2D WISE NMR

One can simultaneously probe the chain conformation and mobility using the 2D wide-line separation (WISE) NMR experiment. This experiment plots ^{13}C chemical shifts (which are sensitive to chain conformation) versus wide-line ^1H spectra (which are sensitive to molecular motion). For example, the 1D ^{13}C NMR spectra, along with the proton line shapes extracted from 2D WISE spectra of octadecylphosphonic acid (ODPA) adsorbed on different metal oxide powders, are shown in Figure 4.[39a] Whereas the ^1H slices for the all-trans chains of ODPA/Zr_2O_3 and ODPA/TiO_2 display reduced solid-state proton line widths, ODPA adsorbed on γ-Al_2O_3 exhibits the broad Gaussian proton line shape typical of a rigid crystalline organic solid. This spectrum establishes that, instead of a monolayer, a bulk lamellar aluminophosphonate is formed where the chains are packed into crystalline bilayers.[39a] In contrast, $C_{18}SH$,[10] $C_{18}PO_3H_2$, and $C_{17}CO_2H$[39] monolayers all exhibit the triangular-shaped proton line shapes and reduced line widths (20−35 kHz) which are characteristic of alkyl chains in an intermediate motional state. Populations of disordered chains, as shown in the 2D WISE spectrum of ODPA/TiO_2, display narrow proton line widths of less than 5 kHz. All of these results confirm that, despite different headgroups and substrates, the alkyl chains of the thiol and organic acid SAMs display a very similar motional state.

The detailed mechanism of the chain-disordering process was determined from ^2H NMR spectroscopy of specifically deuterated samples.[9] ^2H NMR is a powerful method for probing the structure and dynamics of ordered systems since the line shapes, dominated by the quadrupolar interaction, are theoretically well understood and depend primarily on the amplitude and symmetry of the

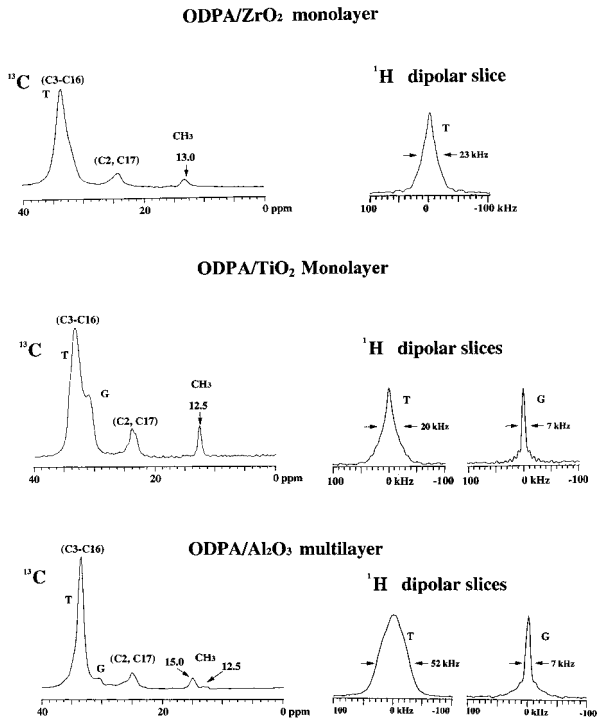

FIGURE 4. Solid-state high-resolution ^{13}C and wide-line ^1H NMR spectra extracted from 2D WISE NMR experiments for octadecylphosphonic acid (ODPA) adsorbed on different metal oxides. The slices in the ^1H dimension corresponding to the transoid (T) and gauchoid (G) ^{13}C methylene signals are shown. (Adapted from ref 39a.)

molecular motions. A low-temperature (−55 °C) ^2H NMR spectrum of $d_8(C_{10}-C_{13})$-labeled $C_{18}S$/Au nanoparticles is characteristic (quadrupole splitting of 118 kHz) of C−D bonds having very little motion. At −30 °C, this ^2H spectrum evolves to become a "flat-topped" peak, a line shape attributed to restricted trans−gauche isomerization. Near the phase transition temperature of 50 °C, the broad component abruptly disappears and above 50 °C only a narrow isotropic peak associated with extensive motion remains.[9] By contrast, the ^2H resonance of the C_1-deuterated chains remains a broad Pake pattern at temperatures up to 65 °C. This establishes that, on the microsecond time scale probed by ^2H NMR spectroscopy, (i) the C_1-C_2 bond does not experience a measurable degree of trans−gauche bond isomerization, (ii) it is unlikely that the RS chain undergoes axial rotation about the C−S bond, and (iii) there is no diffusion of the RS/Au species on the Au particle surface. Overall, the temperature dependence of the ^2H NMR spectra, ^{13}C relaxation measurements, and CD_2 stretching frequencies indicates that the chain disordering originates in the chain ends and propagates toward the middle of the chain. This motional disordering does not, however, extend as far as the sulfur headgroup.[9] Solid-state ^{13}C and ^{31}P 2D exchange NMR experiments, designed to detect "ultraslow" motions, demonstrate that the headgroups of alkanoate and alkanephosphonate monolayers also remain fixed and motionless above the chain-disordering temperatures.[39c]

These dynamics studies of 3D SAMs agree with molecular dynamics simulations of densely packed $C_{15}S$/Au

2D SAMs which predict that the formation of internal gauche defects in these assemblies is coupled to the onset of axial rotation.[3] Recent molecular dynamics studies of the RS/Au 3D SAMs closely concur with the ^{2}H NMR results and even agree with the "melting" transition temperatures observed experimentally.[43]

Modulation of Chain Dynamics with H-Bonding End Groups

SAMs with alcohol and carboxylic acid terminal groups have been used for the development of chemical sensors, the immobilization of proteins, and further chemical derivatization. Although the conformational order and intramonolayer hydrogen bonding are essential to these applications, these structural features are not well characterized. SAMs with a weakly hydrogen bonded OH terminal group, $HO(CH_2)_{16}S/Au$[10] and $HO(CH_2)_{15}CO_2/ZrO_2$,[39c] in fact, exhibit chain order and dynamics similar to those of CH_3-terminated monolayers. The only difference in the properties is a modest raising of the order−disorder transition temperature relative to that of the methyl-terminated SAM of the same chain length. The strongly hydrogen bonding group, CO_2H, on the other hand, induces conformational order in RS/Au chains which are otherwise too short to order via van der Waals interactions alone.[44] Moreover, the dynamic behavior of HO_2C-C_7S/Au 3D SAMs is radically different from that of the HO- and CH_3-terminated SAMs. The wide-line ^{1}H NMR spectrum of HO_2C-C_7S/Au exhibits a broad Gaussian proton line shape characteristic of a rigid crystalline organic solid. The C_8S/Au 3D SAM is disordered at 300 K, but chain disordering in HO_2C-C_7S/Au only begins at 415 K. There is a marked hysteresis in the HO_2C-C_7S/Au case as, upon cooling, the chain-reordering process is very slow—on the order of weeks.[44] Both H-bonded and free CO_2H groups are detected by vibrational spectroscopy in RS/Au 2D SAMs, while in the 3D SAM case there is more extensive H-bonding. The pronounced thermal hysteresis is perhaps due to the formation of interparticle as well as intramonolayer hydrogen bonds in the 3D HO_2C-C_7S/Au nanoparticle SAMs. We are currently testing this conjecture by studying CO_2H-terminated SAMs on larger diameter particles, which will serve to reduce the extent of interparticle hydrogen bonding.

Overview

Our spectroscopic and calorimetric studies of SAMs demonstrate that self-assembled monolayers do, indeed, have a rich dynamics. The dynamic features of these systems are the following:

(i) The monolayers are in a gel-like state below the order−disorder temperature with a pronounced motional gradient along the alkyl chains.

(ii) Reversible, chain-length-dependent order−disorder transitions occur; the headgroups (thiolate, carboxylate, or phosphonate) remain immobile.

(iii) Polar functional groups can dramatically alter the temperatures and kinetics of these transitions.

(iv) The electrochemical detection of transitions at the same temperatures for RS/Au SAMs supports the existence of a similar dynamic state in planar 2D SAMs.

The implications of observing parallel phenomena in 2D and 3D SAMs are exciting since they indicate that these systems are excellent models of membranes. To this end, we are currently exploring ways of triggering trans-SAM ion fluxes through chemical rather than thermal stimulation.Throughout this Account we have noted parallels between phospholipid dynamics in membranes and the SAM systems. Different experimental techniques, when applied to the lipid membrane systems, often seem to yield "different" pictures.[45] These differences, however, invariably reflect different spectroscopic time scales. Of importance, of course, is whether the technique used reports the superposition of individual events or the averaging of events over a well-defined period, and how well the technique can discriminate between two or more "states". When these considerations are accounted for, a reasonably convergent description of phase and dynamics is found in lipid systems. Such a convergent description is just beginning to develop in the SAM literature as well.

We acknowledge the many contributions of our co-workers and collaborators: W. Gao, L. M. Demers, L. Dickinson, Dr. F. Morin, C. Grozinger, S. Pawsey, H. Schmitt, L. Cuccia, S. Singh, F. Bensebaa, R. Back, Prof. T. Ellis, and Prof. G. R. Brown. A.B. is a recipient of a NSERC Doctoral Fellowship. This work was supported by NSERC Research (L.R., R.B.L.) and FCAR Equipe Grants (L.R.).

References

(1) Bishop, A. R.; Nuzzo, R. G. Self-assembled-monolayers: recent developments and applications. *Curr. Opin. Colloid Interface Sci.* **1996**, *1*, 127.

(2) Ulman, A. Formation and Structure of Self-Assembled Monolayers. *Chem. Rev.* **1996**, *96*, 1533.

(3) (a) Mar, W.; Klein, M. L. Molecular dynamics study of the self-assembled monolayer composed of $S(CH_2)_{14}CH_3$ molecules using an all-atoms model. *Langmuir* **1994**, *10*, 188. (b) Hautman, J.; Klein, M. L. Molecular-dynamics simulation of the effects of temperature on a dense monolayer of long-chain molecules. *J. Chem. Phys.* **1990**, *93*, 7483. (c) Hautman, J.; Bareman, J. P.; Mar, W.; Klein, M. L. Molecular dynamics investigations of self-assembled monolayers. *J. Chem. Soc., Faraday Trans.* **1991**, *87*, 2031.

(4) Badia, A.; Back, R.; Lennox, R. B. Electrochemical detection of phase transitions in self-assembled monolayers. *Angew. Chem., Int. Ed. Engl.* **1994**, *33*, 2332.

(5) Brust, M.; Walker, M.; Bethell, D.; Schiffrin, D. J.; Whyman, R. Synthesis of thiol-derivatized gold nanoparticles in a two-phase liquid−liquid system. *J. Chem. Soc., Chem. Commun.* **1994**, 801.

(6) Badia, A.; Singh, S.; Demers, L.; Cuccia, L.; Brown, G. R.; Lennox, R. B. Self-assembled monolayers on gold nanoparticles. *Chem. Eur. J.* **1996**, *2*, 359.

(7) Terrill, R. H.; Postlethwaite, T. A.; Chen, C.-H.; Poon, C.-D.; Terzis, A.; Chen, A.; Hutchison, J. E.; Clark, M. R.; Wignall, G.; Londono, J. D.; Superfine, R.; Falvo, M.; Johnson, C. S., Jr.; Samulski, E. T.; Murray, R. W. Monolayers in Three Dimensions: NMR, SAXS, Thermal, and Electron Hopping Studies of Alkanethiol Stabilized Gold Clusters. *J. Am. Chem. Soc.* **1995**, *117*, 12537.

(8) Hostetler, M. J.; Stokes, J. J.; Murray, R. W. Infrared Spectroscopy of Three-Dimensional Self-Assembled Monolayers: N-Alkanethiolate Monolayers on Gold Cluster Compounds. *Langmuir* **1996**, *12*, 3604.

(9) Badia, A,; Cuccia L.; Demers L.; Morin, F.; Lennox, R. B. Structure and Dynamics in Alkanethiolate Monolayers Self-Assembled on Gold Nanoparticles: A DSC, FT-IR, and Deuterium NMR Study. *J. Am. Chem. Soc.* **1997**, *119*, 2682.

(10) (a) Gao, W.; Reven, L. Solid-State NMR Studies of Self-Assembled Monolayers. *Langmuir* **1995**, *11*, 1860. (b) Badia, A.; Gao, W.; Singh, S.; Demers, L.; Cuccia, L.; Reven, L. Structure and Chain

Dynamics of Alkanethiol-Capped Gold Colloids. *Langmuir* **1996**, *12*, 1262.
(11) Siloxane SAMs will not be described here, as both their self-assembly and final structure are intrinsically different from the thiol and organic acid monolayers. Whereas the latter form monolayers because of the correspondence between the substrate and the surfactant, the siloxanes may cross-link prior to, or after, adsorption. See, for example: Allara, D. L.; Parikh, A. N.; Rondelez, F. Evidence for a Unique Chain Organization in Long Chain Silane Monolayers Deposited on Two Widely Different Solid Substrates. *Langmuir* **1995**, *11*, 2357.
(12) Marsh, D. *Handbook of Lipid Bilayer Membranes*; CRC Press: Boca Raton, FL, 1991; pp 135−150.
(13) Edinger, K.; Goelzhaeuser, A.; Demota, K.; Woell, C.; Grunze, M. Formation of self-assembled monolayers of n-alkanethiols on gold: a scanning tunneling microscopy study on the modification of substrate morphology. *Langmuir* **1993**, *9*, 4.
(14) (a) Delamarche, E.; Michel, B.; Biebuyck, H. A.; Gerber, C. Golden interfaces. The surface of self-assembled monolayers. *Adv. Mater.* **1996**, *8*, 719. (b) Delamarche, E.; Michel, B.; Gerber, Ch.; Anselmetti, D.; Guentherodt, H.-J.; Wolf, H.; Ringsdorf, H. Real-Space Observation of Nanoscale Molecular Domains in Self-Assembled Monolayers. *Langmuir* **1994**, *10*, 2869.
(15) (a) Poirier, G. E.; Tarlov, M. J. The c(4×2) Superlattice of n-Alkanethiol Monolayers Self-Assembled on Au(111). *Langmuir* **1994**, *10*, 2853. (b) Poirier, G. E. Coverage-Dependent Phases and Phase Stability of Decanethiol on Au(111). *Langmuir* **1999**, *4*, 1167.
(16) Schoenenberger, C.; Jorritsma, J.; Sondag-Huethorst, J. A. M.; Fokkink, L. G. J. Domain Structure of Self-Assembled Alkanethiol Monolayers on Gold. *J. Phys. Chem.* **1995**, *99*, 3259.
(17) (a) Porter, M. D.; Bright, T. B.; Allara, D. L.; Chidsey, C. E. D. Spontaneously organized molecular assemblies. 4. Structural characterization of n-alkyl thiol monolayers on gold by optical ellipsometry, infrared spectroscopy, and electrochemistry. *J. Am. Chem. Soc.* **1987**, *109*, 3559. (b) Nuzzo, R. G.; Dubois, L. H.; Allara, D. L. Fundamental studies of microscopic wetting on organic surfaces. 1. Formation and structural characterization of a self-consistent series of polyfunctional organic monolayers. *J. Am. Chem. Soc.* **1990**, *112*, 558.
(18) (a) Camillone, N.; Chidsey, C. E. D.; Liu, G. Y.; Putvinski, T. M.; Scoles, G. Surface structure and thermal motion of n-alkane thiols self-assembled on gold(111) studied by low-energy helium diffraction. *J. Chem. Phys.* **1991**, *94*, 8493. (b) Chidsey, C. E. D.; Liu, G. Y.; Rowntree, P.; Scoles, G. Molecular order at the surface of an organic monolayer studied by low energy helium diffraction. *J. Chem. Phys.* **1989**, *91*, 4421.
(19) Dubois, L. H.; Zegarski, B. R.; Nuzzo, R. G. Temperature induced reconstruction of model organic surfaces. *J. Electron Spectrosc. Relat. Phenom.* **1990**, *54/55*, 1143.
(20) Bensebaa, F.; Ellis, T. H.; Badia, A.; Lennox, R. B. Thermal Treatment of n-Alkanethiolate Monolayers on Gold, As Observed by Infrared Spectroscopy. *Langmuir* **1998**, *14*, 2361.
(21) Fenter, P.; Eisenberger, P.; Liang, K. S. Chain-length dependence of the structures and phases of alkanethiols ($CH_3(CH_2)_{n-1}SH$) self-assembled on gold(111). *Phys. Rev. Lett.* **1993**, *70*, 2447.
(22) Camillone, N.; Eisenberger, P.; Leung, T. Y. B.; Schwartz, P.; Scoles, G.; Poirier, G. E.; Tarlov, M. J. New monolayer phases of n-alkane thiols self-assembled on Au(111): preparation, surface characterization, and imaging. *J. Chem. Phys.* **1994**, *101*, 11031.
(23) Poirier, G. E.; Tarlov, M. J. Molecular ordering and gold migration observed in butanethiol self-assembled monolayers using scanning tunneling microscopy. *J. Phys. Chem.* **1995**, *99*, 10966.
(24) Bucher, J.-P.; Santesson, L.; Kern, K. Thermal Healing of Self-Assembled Organic Monolayers: Hexane- and Octadecanethiol on Au(111) and Ag(111). *Langmuir* **1994**, *10*, 979.
(25) Stranick, S. J.; Parikh, A. N.; Allara, D. L.; Weiss, P. S. A New Mechanism for Surface Diffusion: Motion of a Substrate−Adsorbate Complex. *J. Phys. Chem.* **1994**, *98*, 11136.
(26) (a) Allara, D. L.; Nuzzo, R. G. Spontaneously organized molecular assemblies. 1. Formation, dynamics, and physical properties of n-alkanoic acids adsorbed from solution on an oxidized aluminum surface. *Langmuir* **1985**, *1*, 45. (b) Schlotter, N. E.; Porter, M. D.; Bright, T. B.; Allara, D. L. Formation and structure of a spontaneously adsorbed monolayer of arachidic acid on silver. *Chem. Phys. Lett.* **1986**, *132*, 93.
(27) (a) Tao, Y. T. Structural comparison of self-assembled monolayers of n-alkanoic acids on the surfaces of silver, copper, and aluminum. *J. Am. Chem. Soc.* **1993**, *115*, 4350. (b) Tao, Y. T.; Hietpas, G. D.; Allara, D. L. HCl Vapor-Induced Structural Rearrangements of n-Alkanoate Self-Assembled Monolayers on Ambient Silver, Copper, and Aluminum Surfaces. *J. Am. Chem. Soc.* **1996**, *118*, 6724.
(28) Risse, T.; Hill, T.; Schmidt, J.; Abend, G.; Hamann, H.; Freund, H.-J. Investigation of the Molecular Motion of Self-Assembled Fatty Acid Films. *J. Phys. Chem. B* **1998**, *102*, 2668.
(29) Cao, G.; Hong, H. G.; Mallouk, T. E. Layered metal phosphates and phosphonates: from crystals to monolayers. *Acc. Chem. Res.* **1992**, *25*, 420.
(30) (a) Woodward, J. T.; Schwartz, D. K.. In Situ Observation of Self-Assembled Monolayer Growth. *J. Am. Chem. Soc.* **1996**, *118*, 7861. (b) Woodward, J. T.; Ulman, A.; Schwartz, D. K. Self-Assembled Monolayer Growth of Octadecylphosphonic Acid on Mica. *Langmuir* **1996**, *12*, 3626. (c) Woodward, J. T.; Doudevski, I.; Sikes, H. D.; Schwartz, D. K. Kinetics of Self-Assembled Monolayer Growth Explored via Submonolayer Coverage of Incomplete Films. *J. Phys. Chem. B* **1997**, *101*, 7535.
(31) Bram, C.; Jung, C.; Stratmann, M. Self-assembled molecular monolayers on oxidized inhomogeneous aluminum surfaces. *Fresenius J. Anal. Chem.* **1997**, *358*, 108.
(32) Finklea, H. O. In *Electroanalytical Chemistry*; Bard, A. J., Rubinstein, I., Eds.; Marcel Dekker Inc.: New York, 1996; Vol. 19, pp 109−335.
(33) Forouzan, G.; Bard, A. J.; Mirkin, M. V. Voltammetric and scanning electrochemical microscopic studies of the adsorption kinetics and self-assembly of n-alkanethiol monolayers on gold. *Isr. J. Chem.* **1997**, *37*, 155.
(34) (a) Papahadjopoulos, D.; Jacobson, K.; Nir, S.; Isaac, T. Phase transitions in phospholipid vesicles. Fluorescence polarization and permeability measurements concerning the effect of temperature and cholesterol. *Biochim. Biophys. Acta* **1973**, *311*, 330. (b) Corvera, E.; Mouritsen, O. G.; Singer, M. A.; Zuckermann, M. J. The permeability and the effect of acyl-chain length for phospholipid bilayers containing cholesterol: theory and experiment. *Biochim. Biophys. Acta* **1992**, *1107*, 261. (c) Mouritsen, O. G.; Jorgensen, K. Small-scale lipid-membrane structure: simulation versus experiment. *Curr. Opin. Struct. Biol.* **1997**, *7*, 518.
(35) Naselli, C.; Rabolt, J. F.; Swalen, J. D. Order−disorder transitions in Langmuir−Blodgett monolayers. I. Studies of two-dimensional melting by infrared spectroscopy. *J. Chem. Phys.* **1985**, *82*, 2136.
(36) Camillone, N.; Eisenberger, P.; Leung, T. Y. B.; Schwartz, P.; Scoles, G.; Poirier, G. E.; Tarlov, M. J. New monolayer phases of n-alkane thiols self-assembled on Au(111): preparation, surface characterization, and imaging. *J. Chem. Phys.* **1994**, *101*, 11031.
(37) Hostetler, M. J.; Murray, R. W. Colloids and self-assembled monolayers. *Curr. Opin. Colloid Interface Sci.* **1997**, *2*, 42.
(38) Whetten, R. L.; Khoury, J. T.; Alvarez, M. M.; Murthy, S.; Vezmar, I.; Wang, Z. L.; Stephens, P. W.; Cleveland, C. L.; Luedtke, W. D.; Landman, U. Nanocrystal gold molecules. *Adv. Mater.* **1996**, *8*, 428.
(39) (a) Gao, W.; Dickinson, L.; Grozinger, C.; Morin, F. G.; Reven, L. Self-assembled monolayers of alkylphosphonic acids on metal oxides. *Langmuir* **1996**, *12*, 6429. (b) Gao, W.; Dickinson, L.; Grozinger, C.; Morin, F. G.; Reven, L. Order−disorder transitions in self-assembled monolayers: A ^{13}C solid-state NMR study. *Langmuir* **1997**, *13*, 115. (c) Pawsey, S.; Yach, K.; Halla, J.; Reven, L. Self-assembled monolayers of alkanoic acids: A solid-state NMR study. *Langmuir*, in press. (d) Reven, L., Dickinson, L. NMR spectroscopy of self-assembled monolayers. *Thin Films* **1998**, *24*, 149.
(40) Weast, R. C. *CRC Handbook of Chemistry and Physics*, 70th ed.; CRC Press: Boca Raton, FL, 1989−90.
(41) Riegler, J. E. Thermal behavior of Langmuir−Blodgett films. 1. Electron diffraction studies on monolayers of cadmium stearate, arachidate, and behenate. *J. Phys. Chem.* **1989**, *93*, 6475.
(42) Bayerl, T. M.; Bloom, M. Physical properties of single phospholipid bilayers adsorbed to micro glass beads. A new vesicular model system studied by deuterium nuclear magnetic resonance. *Biophys. J.* **1990**, *58*, 357.
(43) (a) Luetke, W. D.; Landman, U. Structure, dynamics, and thermodynamics of passivated gold nanocrystallites and their assemblies. *J. Phys. Chem.* **1996**, *100*, 13323. (b) Luetke, W. D.; Landman, U. Structure and thermodynamics of self-assembled monolayers on gold nanocrystallites. *J. Phys. Chem B* **1998**, *102*, 6566.
(44) Schmitt, H.; Badia, A.; Dickinson, L.; Reven, L.; Lennox, R. Bruce. The effect of terminal hydrogen bonding on the structure and dynamics of nanoparticle self-assembled monolayers (SAMs). An NMR dynamics study. *Adv. Mater.* **1998**, *10*, 475.
(45) Bloom, M.; Thewalt, J. Spectroscopic determination of lipid dynamics in membranes. *Chem. Phys. Lipids* **1994**, *73*, 27.

AR9702841